Supplementary Material

Title: Natural killer cells suppress cancer metastasis by eliminating circulating cancer cells

Maulik Vyas[1], Marta Requesens[1], Thao H. Nguyen[1], Domitille Peigney[1], Marjan Azin[1], Shadmehr Demehri[1]*

SUPPLEMENTARY FIGURES

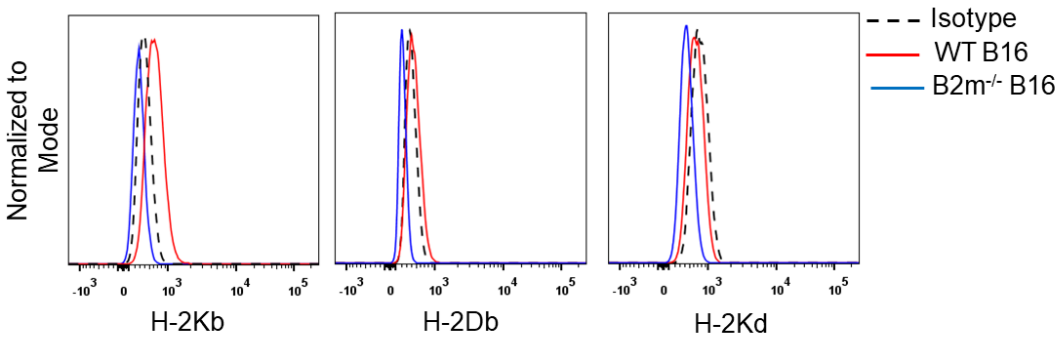

Figure S1. MHC-I expression on WT and B2m$^{-/-}$ B16 cells. The expression of MHC-I alloantigens H-2Kb (C57BL/6), H-2Db (C57BL/6) and H-2Kd (BALB/c) were examined on the surface of WT and B2m$^{-/-}$ B16 melanoma cells.

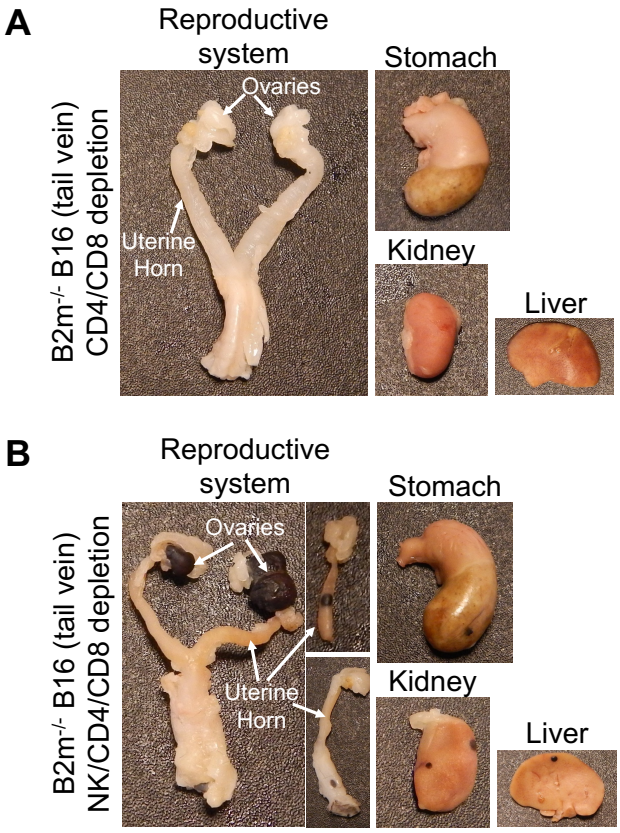

Figure S2. NK and T cell depletion results in extrapulmonary metastases of B16 melanoma. **(A, B)** Representative macroscopic images of extrapulmonary metastases of $B2m^{-/-}$ B16 melanoma following tail vein IV injection and treatment with anti-CD4/CD8 (A) and anti-NK1.1/CD4/CD8 (B) antibodies.

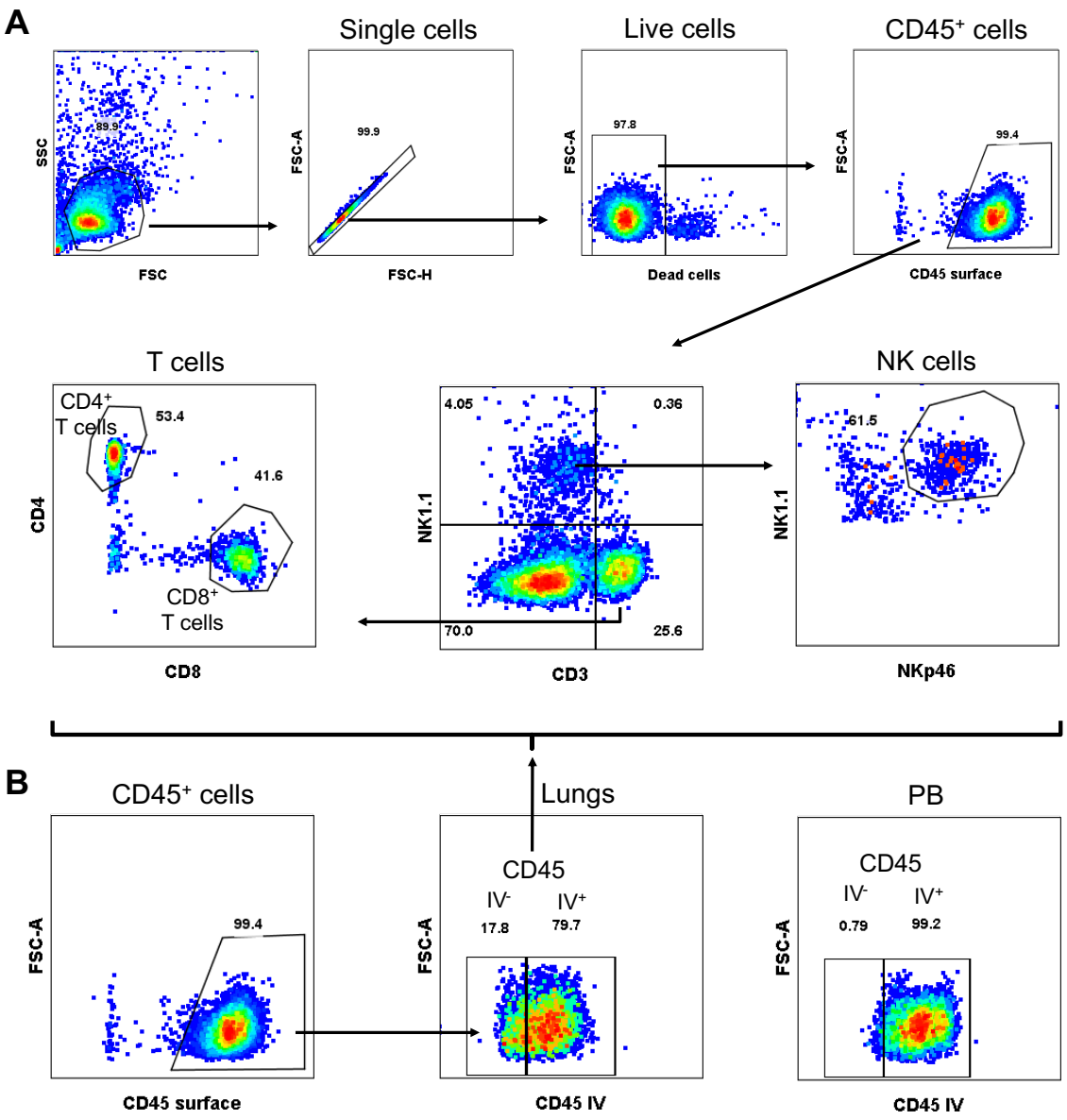

Figure S3. Gating strategy to detect total and tissue infiltrating (IV^{neg}) NK and T cells. For specific evaluation of the immune cells infiltrating into the lung tissue, fluorescently labeled anti-CD45 antibody was intravenously administered to mice 3 minutes before organ harvest. CD45-stained immune cells from the vasculature are termed as CD45 IV^+ while tissue-resident/emigrated immune cells which remained unstained by intravenously injected CD45 antibody are termed as CD45 IV^-. Following the organ harvest, immune cells were *ex vivo* stained by distinctly labeled CD45 antibody ("CD45 surface") to stain all immune cells. **(A)** Total $CD45^+$

immune cells gated among forward/side scatter-based singlets gate followed by fixable live/dead stain negative live cells gate. Total NK cells were subsequently detected by gating for $CD3^-$, $NK1.1^+$, $NKp46^+$ population. Total $CD4^+$ and $CD8^+$ T cells were detected by gating for $NK1.1^-$, $CD3^+$, $CD4^+$ or $CD8^+$ populations. **(B)** To detect circulating versus tissue-infiltrating immune cells in the lung, total *ex vivo* labeled $CD45^+$ immune cells were gated for CD45 IV^+ (IV^{pos}) and CD45 IV^- (IV^{neg}) populations accounting for circulating and tissue-infiltrating immune cells. The gating of CD45 IV^+ (IV^{pos}) and CD45 IV^- (IV^{neg}) immune cells among total $CD45^+$ cells was generated based on the peripheral blood (PB) sample where all $CD45^+$ immune cells were CD45 IV^+ (IV^{pos}) (i.e., fluorescently labeled by intravenously injected CD45 antibody). CD45 IV^- (IV^{neg}) NK cells and $CD4^+$/$CD8^+$ T cells were further detected as described in (A).

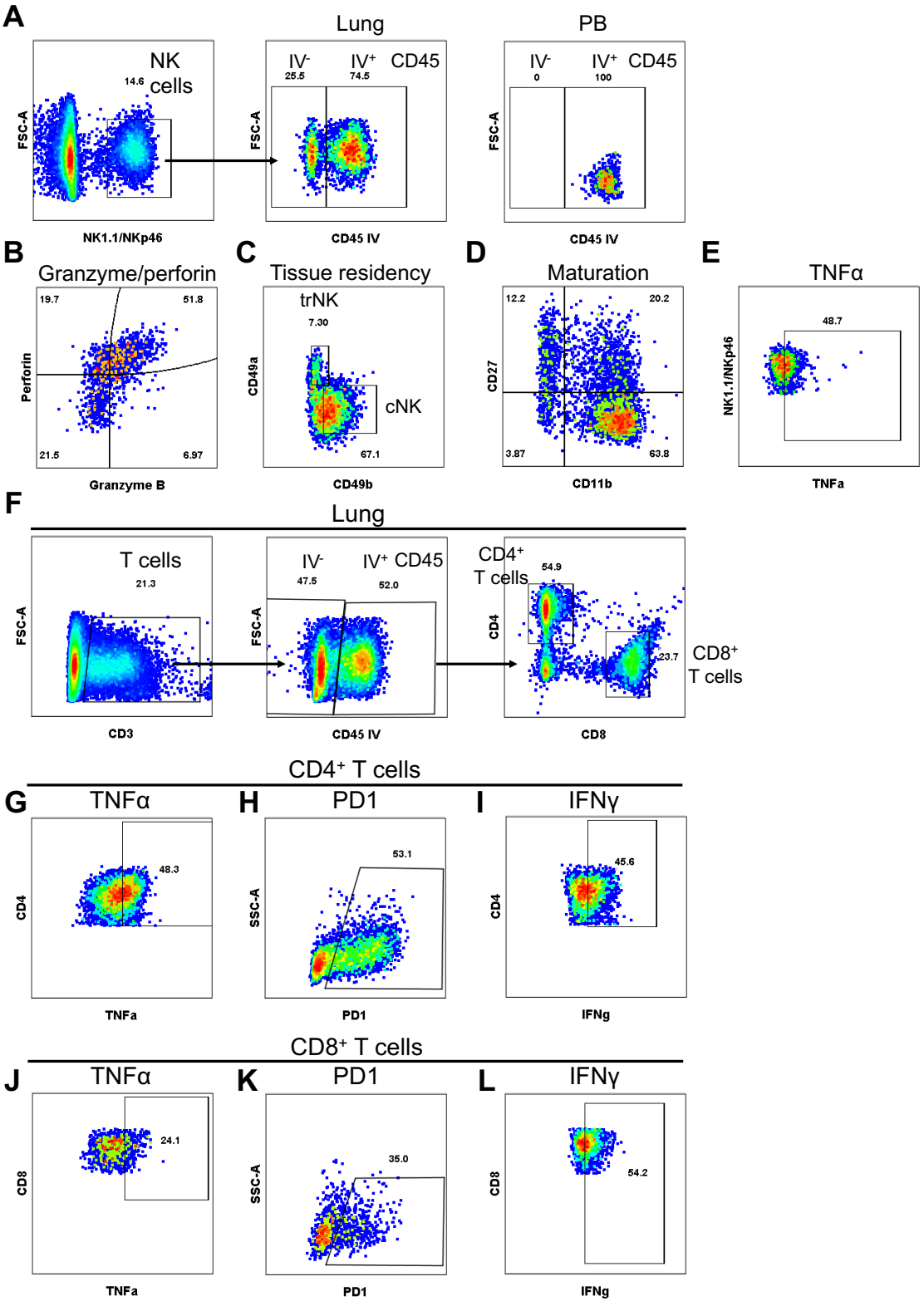
A
Lung
PB
NK cells
14.6
IV- IV+ CD45
25.5 74.5
IV- IV+ CD45
0 100
FSC-A
NK1.1/NKp46
CD45 IV
B
Granzyme/perforin
19.7 51.8
21.5 6.97
Perforin
Granzyme B
C
Tissue residency
trNK
7.30
cNK
CD49a
67.1
CD49b
D
Maturation
12.2 20.2
3.87 63.8
CD27
CD11b
E
TNFα
48.7
NK1.1/NKp46
TNFa
F
Lung
T cells
21.3
IV- IV+ CD45
47.5 52.0
CD4+ T cells
54.9
23.7
CD8+ T cells
FSC-A
CD3
CD45 IV
CD4
CD8
CD4+ T cells
G
TNFα
48.3
H
PD1
53.1
I
IFNγ
45.6
CD4
TNFa
SSC-A
PD1
IFNg
CD8+ T cells
J
TNFα
24.1
K
PD1
35.0
L
IFNγ
54.2
CD8
TNFa
SSC-A
PD1
IFNg

Figure S4. Gating strategy for functional characterization of Lung IV^{pos} and IV^{neg} NK and T cells. (A) NK cells detected by gating for $CD3^-$, NK1.1/ $NKp46^+$ population. To detect circulating versus tissue-infiltrating immune cells, mice were intravenously injected with fluorescently labeled CD45 antibody 3 minutes before organ harvest to fluorescently label all $CD45^+$ immune cells in the vasculature. The gating of CD45 IV^+ (IV^{pos}) and CD45 IV^- (IV^{neg}) NK cells among total NK cells was generated based on the peripheral blood (PB) sample where all NK cells were CD45 IV^+ (IV^{pos}) (i.e., fluorescently labeled by intravenously injected CD45 antibody). **(B-E)** CD45 IV^+ (IV^{pos}) and CD45 IV^- (IV^{neg}) lung NK cells gated for granzyme B/perforin (B), CD49b/CD49a (C), CD11b/CD27 (D), and TNFα (E) based on the Fluorescence Minus One (FMO) controls. **(F)** T cells detected by gating for $CD3^+$, NK1.1/ $NKp46^-$ population. The gating of CD45 IV^+ (IV^{pos}) and CD45 IV^- (IV^{neg}) T cells was generated as for NK cells and were subsequently gated for $CD4^+$ and $CD8^+$ T cells. **(G-L)** CD45 IV^+ (IV^{pos}) and CD45 IV^- (IV^{neg}) lung $CD4^+$ (G, H, I) and $CD8^+$ (J, K, L) T cells were further gated for TNFα (G, J), PD1 (H, K), and IFNγ (I, L) based on the FMO controls.

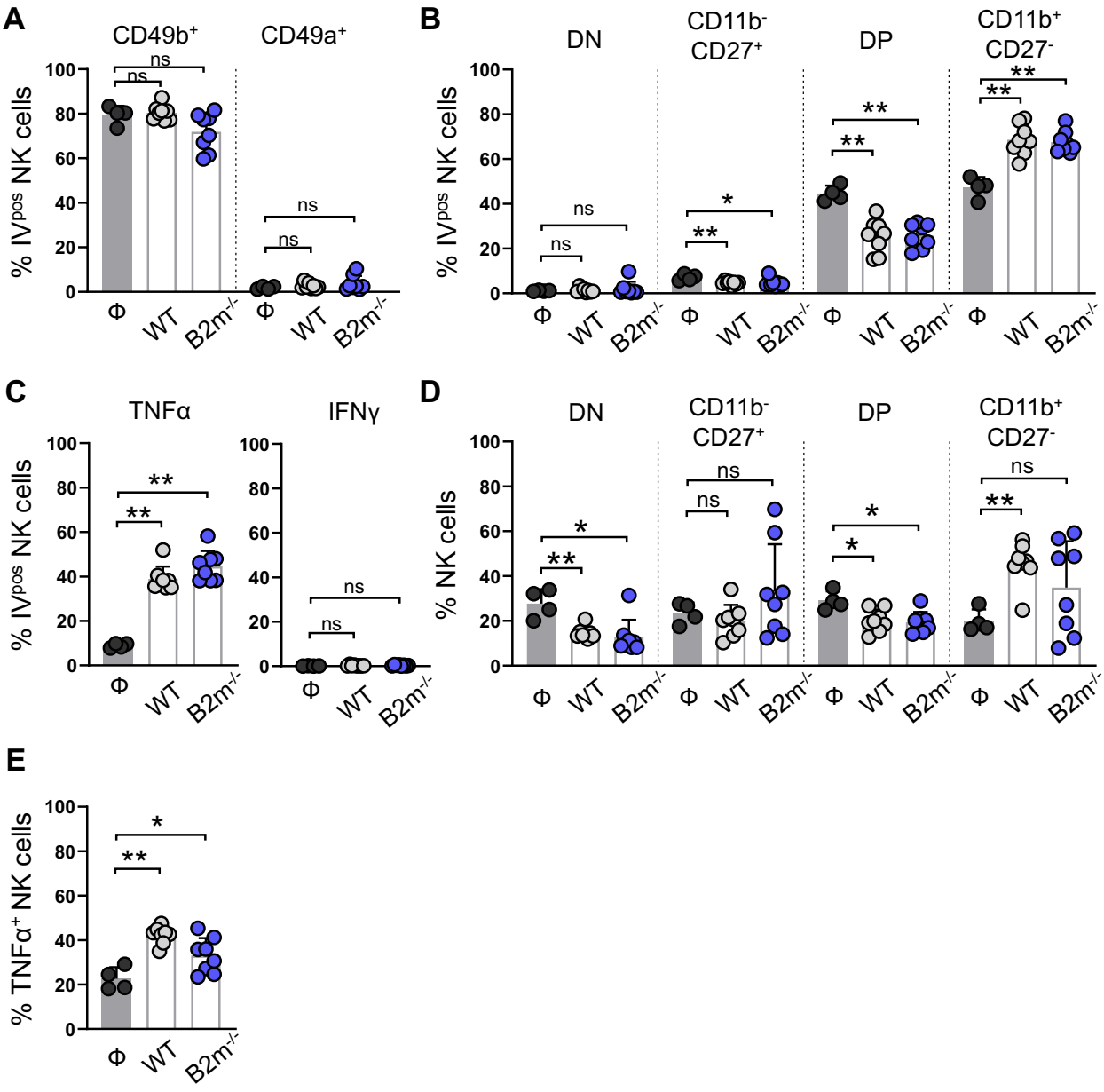

Figure S5. Characterization of lung and liver NK cells in response to metastatic melanoma. **(A)** Quantification of conventional ($CD49b^+$) and tissue-resident ($CD49a^+$) circulating (IV^{pos}) NK cells in the lung at day 14 after WT B16 (WT) and $B2m^{-/-}$ B16 ($B2m^{-/-}$) melanoma tail vein IV injection in comparison with untreated mice (Φ). **(B)** Quantification of maturation status defined by CD11b and CD27 expression in circulating (IV^{pos}) NK cells in the lung at day 14 after WT B16 (WT) and $B2m^{-/-}$ B16 ($B2m^{-/-}$) melanoma tail vein IV injection in comparison with untreated mice

(Φ). **(C)** Quantification of $TNF\alpha^+$ and $IFN\gamma^+$ circulating (IV^{pos}) NK cells in the lung at day 14 after WT B16 (WT) and $B2m^{-/-}$ B16 ($B2m^{-/-}$) melanoma tail vein IV injection in comparison with untreated mice (Φ). **(D)** Quantification of maturation status defined by CD11b and CD27 expression in liver NK cells at day 14 after WT B16 (WT) and $B2m^{-/-}$ B16 ($B2m^{-/-}$) melanoma tail vein IV injection in comparison with untreated mice (Φ). **(E)** Quantification of $TNF\alpha^+$ liver NK cells at day 14 after WT B16 (WT) and $B2m^{-/-}$ B16 ($B2m^{-/-}$) melanoma tail vein IV injection in comparison with untreated mice (Φ). n = 4-8 mice per group. Graphs show mean + SD. Mann-Whitney *U* test, ns: not significant, * $p < 0.05$, ** $p < 0.01$.

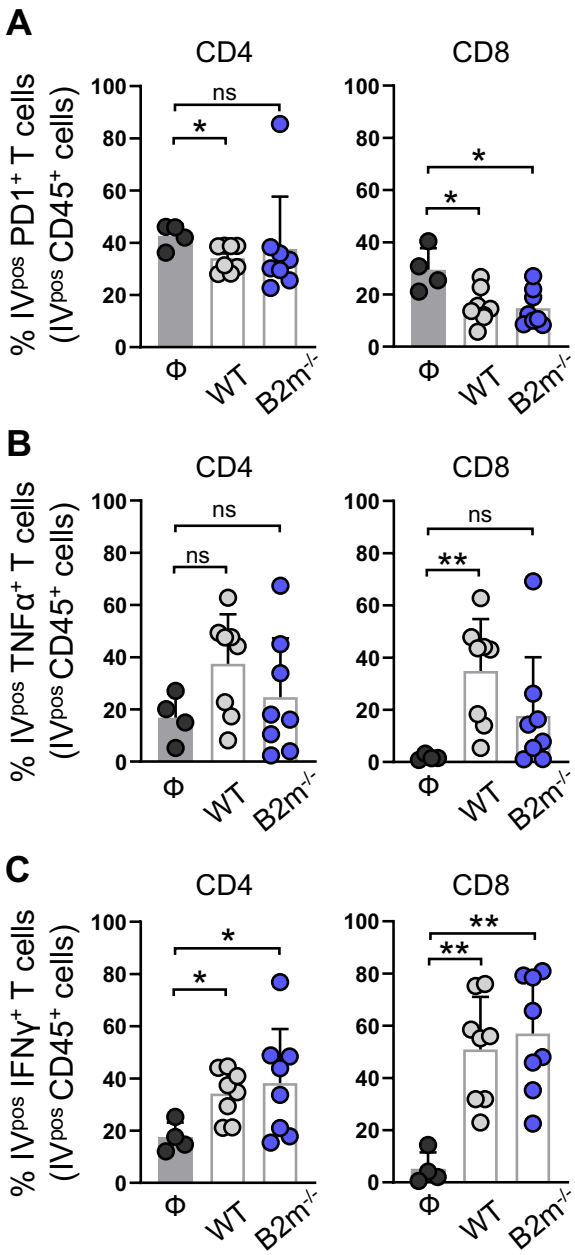

Figure S6. Characterization of circulating T cells in the lung in response to metastatic melanoma. (A-C) Quantification of $PD1^+$ (A), $TNF\alpha^+$ (B), and $IFN\gamma^+$ (C) circulating (IV^{pos}) $CD4^+$ and $CD8^+$ T cells in the lung at day 14 after WT B16 (WT) and $B2m^{-/-}$ B16 ($B2m^{-/-}$) melanoma tail vein IV injection in comparison with untreated mice (Φ). n = 4-8 mice per group. Graphs show mean + SD. Mann-Whitney *U* test, ns: not significant, * $p < 0.05$, ** $p < 0.01$.

SUPPLEMENTARY TABLE

Table S1. Antibodies used for immune cell analysis.

Immunostaining Antibodies	**Clone**	**Company**
Rat Anti-Mouse CD3	CD3-12	Abcam, Cambridge, MA
Rabbit Anti-Mouse CD8	D4W2Z	Cell Signaling Technology, Danvers, MA
Rabbit Anti-Mouse CD4	EPR19514	Abcam
Secondary Antibodies and staining kits		
Goat anti-Rat IgG, Alexa Fluor® 568 conjugate		Thermo Fisher Scientific, Waltham, MA
Goat anti-Rabbit IgG, Alexa Fluor® 488 conjugate		Thermo Fisher Scientific
Flow Cytometry Antibodies		
Mouse		
CD3-BUV395	145-2C11	BioLegend
CD3-APC-Cy7	145-2C11	BioLegend
CD3-PerCP-Cy5.5	145-2C11	BioLegend
CD4-APC-Cy7	GK1.5	BioLegend
CD4-eF450	GK1.5	BioLegend
CD4-PerCP-Cy5.5	GK1.5	BioLegend
CD8-PE	53-6.7	BioLegend
CD8-APC-Cy7	53-6.7	BioLegend
CD8-BUV395	53-6.7	BioLegend
CD45-BV605	30-F11	BioLegend
CD45-APC	30-F11	BioLegend
CD27-PE-Cy7	LG.3A10	BioLegend
Perforin-PE	S16009A	BioLegend
CD19-APC-Cy7	6D5	BioLegend
CD49a-PerCP-Cy5.5	Ha31/8	BioLegend
CD49b-FITC	DX5	BioLegend
NK1.1-APC	PK136	BioLegend
NK1.1-PECy7	PK136	BioLegend
NK1.1-APC-Cy7	PK136	BioLegend
NKp46-APC	29A1.4	BioLegend
NKp46-PE	29A1.4	BioLegend
NKp46-APC-Cy7	29A1.4	BioLegend
CD11b-BUV395	M1/70	eBioscience

PD1-FITC	29F.1A12	BioLegend
IFNγ-eF450	XMG1.2	eBioscience
IFNγ-AF700	XMG1.2	BioLegend
IFNγ-PE-Cy7	XMG1.2	eBioscience
IFNγ-BV605	XMG1.2	BioLegend
TNFα-BV605	MP6-XT22	BioLegend
Granzyme B-AF647	GB11	BioLegend
Granzyme B-Pacific Blue	GB11	BioLegend
H-2Kb-APC	AF6-88.5	BioLegend
H-2Db-PE	KH95	BioLegend
H-2Kd-PE-Cy7	SF1-1.1	BioLegend